Onderstepoort J. vet. Res. 45 (2), 75–92 (1978)

OBSERVATIONS ON THE PATHOLOGY OF CANINE MICROSPORIDIOSIS*

R. M. McCULLY, Col., USAF, VC(1), A. F. VAN DELLEN, Capt., USAF, VC(1), P. A. BASSON(2) and J. LAWRENCE(3)

ABSTRACT

McCULLY, R. M., Col., USAF, VC, VAN DELLEN, A. F., Capt. USAF VC, BASSON, P. A. & LAWRENCE, J., 1978. Observations on the pathology of canine microsporidiosis. *Onderstepoort Journal of Veterinary Research* 45 (2), 75–92 (1978).

The available literature on canine microsporidiosis indicates that this disease, primarily of young dogs, is a distinct clinicopathological entity. It has been confused with canine distemper and rabies, and must be differentiated from toxoplasmosis. Information available on the spectrum of pathological change associated with this disease is incomplete but a distinct pattern emerges from a study of the reports. The aetiological agent appears to have a predilection for the central nervous system and kidneys, but other tissues and organs, and especially the liver, may also be infected. Vasculitis and perivasculitis, which may include fibrinoid necrosis, seem to be a basic lesion. Cellular inflammation ranges from polymorphonuclear leukocyte infiltration in areas of necrosis to focal granulomas. There may be no cellular reaction to compact groups of organisms. Histopathological and ultrastructural studies of this case augment our knowledge of the pathological changes seen with canine microsporidiosis.

Résumé

OBSERVATIONS SUR LA PATHOLOGIE DE LA MICROSPORIDIOSE CANINE

Les publications consacrées à la microsporidiose canine montrent que cette maladie, qui affecte particulièrement les chiots, constitue une entité clinico-pathologique distincte. On l'a confondue avec la maladie de carré et avec la rage, et il faut la distinguer d'avec la toxoplasmose. On ne dispose pas de renseignements complets sur l'éventail des modifications pathologiques liées à cette maladie, mais l'étude des comptes-rendus permet de dégager un schéma distinctif. L'agent étiologique semble avoir une préférence pour le sytème nerveux central et les reins, mais d'autres tissus et organes, notamment le foie, peuvent aussi être infectés. La vasculite et périvasculite, qui peut inclure une nécrose fibrinoïde, semble être une lésion fondamentale. L'inflammation cellulaire varie depuis une infiltration de leucocytes polymorphonucléaires dans les zones de nécrose jusqu'à des granulomes. Il peut ne pas y avoir de réaction cellulaire à des groupes compacts d'organismes. Les études histopathologiques et ultrastructurelles de ce cas augmentent notre connaissance des modifications pathologiques qui se manifestent avec la microsporidiose canine.

INTRODUCTION

The literature on canine microsporidiosis, whether reported as nosematosis or encephalitozoonosis and in association with other diseases (*vide infra*), is not as extensive as that on the disease in rabbits and rodents (Petri, 1969). One confirmed case of nosematosis in a cat (Van Rensburg & Du Plessis, 1971) and one suspected case (Schuster, 1925) indicate that this species is susceptible to infection by microsporidia, though the disease may be rare. Microsporidiosis has seldom been reported in man (Matsubayashi, Koike, Mikata, Takei & Hagiwara, 1959; Margileth, Strano, Chandra, Neafie, Blum & McCully, 1973).

Reported cases of microsporidiosis in the dog suggest that many different cells, tissues and organs can be parasitized by microsporidia but that it has an apparent predilection for the central nervous system and kidneys (Basson, McCully & Warnes, 1966; Kantorowicz & Lewy, 1923; Levaditi, Nicolau & Schoen, 1923; Manouelian & Viala, 1924 & 1927; Perdrau & Pugh, 1930; Petri, 1969; Plowright, 1952; Plowright & Yeoman, 1952). This is so apparent clinicopathologically that Plowright in his excellent report on the pathology of the disease described it as "the encephalitis-nephritis syndrome".

Since the report by Basson *et al.* (1966), nosematosis has been diagnosed fairly frequently on examination of canine tissues submitted to the Veterinary Research Institute, Onderstepoort, and this paper reports in detail the pathological and ultrastructural study of one of these cases.

* The opinions or assertions contained in this report are the private views of the authors and are not to be construed as official or as reflecting the views of the Departments of the Air Force or of Defence.

(1) Geographic Zoonoses Division, Armed Forces Institute of Pathology, Washington D.C. 20306
(2) P.O. Box 81, Grootfontein, South West Africa, 9245
(3) Veterinary Research Laboratory, Salisbury, Rhodesia

Received 9 January 1978—Editor

MATERIALS AND METHODS

A 2–3-months-old Boxer pup born and raised in Rhodesia, was presented clinically as stunted, emaciated and ataxic. At necropsy the only marked change noted was enlargement of the liver.

Kidney, brain, liver, and spinal cord were preserved in 10% formalin. Paraffin sections for light microscopy were stained with haematoxylin and eosin (HE) and various other special stains (Luna, 1960), including Gram's [Brown Brenn (BB) & Humberstone], Giemsa's, periodic acid-Schiff (PAS), Warthin-Starry's (WS), Ziehl-Neelsen's (ZN), and Grocott's (GMS) stains.

For electron microscopy, 0,5–1,0 mm³ blocks of tissue from formalin-fixed specimens were post-fixed in 2% osmium tetroxide, dehydrated in an ethanol gradient and embedded in Epon 812. For tissue orientation, 1–2 μm sections were cut, and stained by Chang's method of staining plastic sections with HE (Chang, 1972). A modified PAS stain was applied to selected sections (Van Dellen, 1974, unpublished observation). Silver sections (60 nm) were cut with a Porter-Blum ultra microtome, mounted on 200 mesh copper grids, stained with 1% aqueous uranyl acetate at 60 °C and Reynold's lead citrate at room temperature, and viewed with a Siemens I-A Elmiskop electron microscope.

MICROSCOPIC FINDINGS

Kidney

Particularly noteworthy was the extremely large number of microsporidia present in all the tissues examined. These organisms were especially numerous in the epithelium and lumen of tubules in the renal medulla and cortex, the capillaries of the glomerular tuft (Fig. 1 & 2), the parietal layer of Bowman's membrane and the interstitium of both cortex and medulla, where they occurred both free and in compact groups. The small blood vessels throughout

the kidney contained microsporidia in their lumina, and many others were present in the media and adventitia of arcuate arteries. The number of organisms in tubular epithelium varied from a few single parasites to large colonies.

The host response varied from virtually none around some of the apparently encysted organisms to an extensive reaction in the vicinity of scattered free microsporidia. In some glomeruli with apparently intact cysts (Fig. 1 & 2) there was no reaction in the glomerular tuft, although Bowman's capsule was surrounded by plasma cells (Fig. 1). In glomeruli where the organisms were partially clumped and partially dispersed, there was mesangial proliferation (Fig. 3 & 4) in response to the scattered microsporidia. In glomeruli containing widely dispersed organisms, there was a marked enlargement of the glomerular tuft. Sometimes such a proliferation of the mesangial cells resulted in a filling of Bowman's space and a synechia between the visceral and parietal layers of Bowman's capsule (Fig. 4). Such glomeruli were frequently surrounded by plasma cells.

In other glomeruli the mesangial proliferation blended with a granulomatous reaction in the parietal layer of Bowman's capsule (Fig. 5). The reaction appeared either to have broken through and merged with an existing reaction or extended as a granulomatous response into the surrounding interstitium (Fig. 6). There was fibrinoid necrosis in some glomerular tufts (Fig. 7). A few polymorphonuclear leucocytes were attracted to necrotic glomeruli (Fig. 8). Some glomeruli seemed contracted and dense (Fig. 9) and were surrounded by an extensive reaction in the adjacent interstitium. Russell-Fuchs bodies were scattered among the plasma cells. Organisms in the arcuate arteries were accompanied by fibrinoid necrosis of the media and adventitia and concentrations of mononuclear cells, especially lymphocytes and plasma cells (Fig. 10). The nodular distribution along the arteries (Fig. 11), together with the other features, made the lesions resemble those of periarteritis nodosa. In the interstitium, microsporidia, surrounded by an apparent membrane, either attracted no host cells (Fig. 12) or only plasma cells, but when free they provoked a granulomatous response, in which histiocytes or epithelioid cells were predominant (Fig. 13). When microsporidia were widely dispersed, the accompanying granulomatous reaction was extensive, sometimes extending directly to a Bowman's capsule containing an apparently non-parasitized glomerular tuft (Fig. 14). A few large cells in areas of affected tubules had multiple nuclei, suggesting that giant cells had formed from the epithelioid or histiocytic cells, though regeneration of tubular epithelium was also a possible explanation. It appeared that some of the tubular epithelial cells ruptured into the lumen (Fig. 15) whereas others ruptured toward the interstitial tissue. In other tubules the lumen appeared greatly narrowed by the distended parasitized epithelial cells (Fig. 16). Some parasitized cells had been shed into the lumen where they could be seen in casts along with other debris, free organisms, and proteinaceous material (Fig. 17). The interstitium of the medulla was densely infiltrated with lymphocytes and plasma cells and scattered numbers of histiocytic or epithelioid cells (Fig. 18). With Gram's stain, intact groups of organisms were well-defined in the glomerular tuft (Fig. 19). The large number of microsporidia in tubular epithelial cells was shown to advantage with either Gram's or Giemsa's stain, the use of which emphasized the number being discharged through the collecting tubules (Fig. 21).

Liver

Microsporidia were present in all areas of the hepatic lobule, and the entire liver was affected. In the wall of some hepatic arteries and both hepatic and portal veins, small spherical spaces, some of which contained microsporidia, were present in the media and adventitia. Apparently, because of the irregular distribution of organisms along vessels, the necrosis and cellular response was nodular and irregular, and occasionally completely circumferential. In cross sections of other vessels only 1 segment of the vessel wall was affected (Fig. 23), but the nodular distribution was better shown in sections containing fairly long, longitudinal views of the vessels. The lesions closely resembled those in the arcuate arteries having focal fibrinoid necrosis (Fig. 22) and mononuclear cell infiltration of the media and adventitia (Fig. 23). Microsporidia were present in groups within the cytoplasm of hepatocytes (Fig. 24) and Kupffer cells, the nuclei of the latter revealing increased basophilia. A number of large, round, multinucleated giant cells were scattered in the sinusoids and were interpreted as being derived from Kupffer cells. Plasma cells were numerous in the sinusoids as well as in portal and periportal areas. Occasionally sinusoids were distended by focal accumulations of polymorphonuclear leucocytes and a few focal granulomas. Closely grouped microsporidia in the cytoplasm of hepatocytes elicited no host response. In a few foci there were collections of as many as 10 contiguous hepatocytes that contained groups of microsporidia. When the free microsporidia were dispersed, microgranulomas consisting of epithelioid cells resulted. Some sinusoids were filled because of Kupffer cell hyperplasia. Free macrophages in some sinusoids were packed with the microsporidia. Other sinusoids were literally filled with the parasites, suggesting that some of the parasitized hepatocytes and Kupffer cells had ruptured. A few multinucleated cells were present in sinusoids and around blood vessels.

Central Nervous System (CNS)

An examination of the frontal and occipital lobes of the cerebral hemispheres, cerebellum, cerebellar peduncles, several levels of medulla oblongata and cervical spinal cord were all virtually equally heavily parasitized with microsporidia and the associated lesions were correspondingly extensive. The cortical areas were severely affected, and large numbers of parasites were present in the zonal layer of the cerebellar hemispheres. There were large groups of microsporidia in Purkinje cells (Fig. 25 & 26) and within other neurons elsewhere in the brain (Fig. 27) and spinal cord (Fig. 28). In the zonal layer of the cerebellum there were large intact groups of microsporidia (Fig. 29) to which there was no host response.

The blood vessels (Fig. 31) contained large numbers of microsporidia which were seen either free in the lumen (Fig. 32 & 34) or within endothelial cells (Fig. 33) and macrophages. The entire lumen of some vessels was packed with microsporidia (Fig. 34), and longitudinal sections of capillaries revealed the organisms arranged in single file. Individual organisms were seen extravascularly in brain substance either adjacent or distant to small visible vessels. Some vessels with no evidence of cellular inflammation were filled with microsporidia (Fig. 31–34). Large mononuclear cells filled the lumen of other vessels, and parasite-laden macrophages formed cuffs around some of the vessels (Fig. 35). Fibrinoid necrosis, similar to that seen in arcuate and hepatic arteries, was also

present in the cerebrospinal arteries (Fig. 36). Some small arteries contained intact intramural groups of microsporidia that elicited no host response. The cerebrum contained long segments of veins, the lumina of which were packed with microsporidia (Fig. 34).

One of the more prominent features of the brain and spinal cord lesions was gliosis subjacent to the pia, but this was even more pronounced in many focal areas and around small blood vessels scattered in both grey and white matter. Gliosis appeared to be composed of fibrous and plump astrocytes and microglia. In various areas of the brain there were large intact groups of microsporidia with apparently no gliosis or other host reaction to them (Fig. 29 & 30). It was evident that scattered individual organisms stimulated the formation of glial nodules (Fig. 37) since they were shown to be plentiful in the nodules when stained with Gram's stain (Fig. 38). The organisms were present in the cytoplasm of individual glial cells and macrophages, as well as free in their vicinity.

The lumina of a few blood vessels in the choroid plexus of the 4th ventricle contained microsporidia. Some vessels showed no host response to the microsporidia, while others contained many mononuclear cells, primarily plasmacytes. There was fibrinoid necrosis of some vessels in the choroid plexus (Fig. 39). Subependymal groups of microsporidia, collections of lymphocytes, and focal gliosis with organisms present among the glial and lymphoid cells were observed. In the medulla oblongata there were glial foci and a number of large neurons containing microsporidia. Focal areas of rarefaction (Fig. 40) and an occasional Russell-Fuchs body (Fig. 41) were found in both grey and white matter of the brain. A few polymorphonuclear leucocytes were seen in response to the focal malacia.

Glial nodules were numerous in the spinal cord and were particularly prominent around blood vessels containing parasites in their lumina. Plasma cells were present in the spinal cord adjacent to parasitized capillaries and groups of microsporidia. Vasculitis and perivascular cuffs were consistently present.

The meninges over the cerebellum were heavily infiltrated by both large and small round cells, and there were many plasma cells and Russell-Fuchs bodies. There were nodular, necrotic inflammatory lesions in the adventitia and media of small arteries (Fig. 42). These were similar to those found in arteries elsewhere in the CNS, the vessels of the liver, and the arcuate arteries in the kidney.

Features of the Organism detected with light Microscopy

The organisms, which stained primarily with the eosin, were fairly easily seen with HE stain and were characterized by a rather refractile appearance. These organisms, and especially those in the kidney, were Gram-positive with the BB and Humberstone stains, blue with Giemsa's stain and acid-fast with ZN. With few exceptions the parasites in neurons and elsewhere in the brain seemed to be almost completely refractory to the ZN stain. Although they were demonstrated with GMS, the WS stain gave more satisfactory results. With PAS the apparently mature spore had positive staining material in the anterior polar vacuole which appeared to coincide with the polaroplast and/or polar cap. A dense PAS-positive central core was evident within apparently immature spores.

The microsporidia in renal tissues were found to be strongly birefringent (Fig. 20). The organisms in neurons, especially in the Purkinje cells, were not birefringent, but elsewhere in the brain an occasional organism polarized.

Ultrastructural findings

With electron microscopy it was established beyond doubt that the organism concerned is a microsporidian parasite since spores containing the typical coiled filament and other ultrastructural features were detectable.

No proliferative forms in the early stage of the parasite's multiplication were demonstrated, but stages in the life cycle from sporont to mature spore and empty spores were found within large cytoplasmic cavitations of the host cell cytoplasm.

The parasites with elongated profiles, irregular, thickened cytoplasmic membranes, and coarse, granular cytoplasm in a somewhat loose arrangement (Fig. 47 & 48) may be sporonts. No developing organellae were discernible in these organisms.

Sporoblasts were very numerous and were usually very electron dense (Fig. 49–54). They were often pyriform, sometimes "cigar shaped", and they consistently revealed an outer, corrugated, angular wall which appeared rough and crenated. The cytoplasmic membrane apparently was not preserved. An electron-translucent zone separated the thin outer wall from the internal components. Organellae of the developing spore, such as the polaroplast with its laminated concentric rings and, in its centre, a cross section of part of the filament, both developing in what will become the anterior pole (Fig. 54—organism on right) were readily discernible at this stage. The developing filament was easily detected in the sporoblast and was the best preserved organelle. The shadow of a single nucleus could be seen in one of the organisms in Fig. 52. Sporoblasts were never seen to be membrane-bound, in pairs, or in a group of any uniform size.

Mature spores measured approximately $0,9 \times 2,4$ μm and possessed 6 loops of filament (Fig. 43–46). The filament was approximately 0,13 nm in diameter and contained a 0,02 nm central electron-dense core (Fig. 43). It was apparently anchored above the polaroplast and under the polar cap which was not well defined (Fig. 44). Traversing posteriorly, the filament formed 6 loops located predominantly in the posterior of the spore. The laminar construction of the polaroplast, located in the anterior vacuole, is clearly revealed in Fig. 44. It appeared that 4 individual laminated polaroplast membranes were radially arranged around the filament traversing the central axis of the polaroplast. The nucleus was present within, but usually above, the major number of coils in the mature spore (Fig. 43). Usually, what appeared to be a single coarse nucleus was seen with difficulty as a shadowy outline (Fig. 43–46). A membrane-bound, homogeneous, irregularly round, indented structure in the posterior pole (Fig. 44) gives the impression of being a nucleus by virtue of its size, shape, and position. Rough endoplasmic reticulum was abundant. Small round densities interpreted as ribosomes on a membrane (not preserved) were seen in a curved or linear pattern (Fig. 44 & 46). There also appeared to be free ribosomes. The bilaminar 0,12 μm thick spore wall consisted of a wide electron-translucent part that extended from the poorly discernible cytoplasmic limiting membrane to the thin outer electron-dense part of the spore wall, which appeared corrugated and sometimes spiralled like a twisted rope.

FIG. 1 Plasma cells adjacent to Bowman's capsule of glomerulus containing a poorly-defined collection of microsporidia. HE × 450

FIG. 2 A higher magnification showing absence of inflammation in a glomerulus containing a collection of microsporidia. HE × 1 600

FIG. 3 Glomerular tuft shows mesangial proliferation of the right side because of dispersal of microsporidia in the capillary loop. HE × 1 250

FIG. 4 Filling of Bowman's space due to proliferation of mesangial cells resulting in a synechia between the visceral and parietal layers of Bowman's membrane. HE × 325

FIG. 5 Mesangial proliferation within glomerulus blending with the granulomatous reaction of Bowman's capsule. HE × 350

FIG. 6 Extension of granulomatous reaction through Bowman's capsule and blending with similar reaction in the interstitium. HE × 100

FIG. 7 Glomerulus showing fibrinoid necrosis on the right side. HE × 250

FIG. 8 Necrosis of glomerulus attracting polymorphonuclear leucocytes surrounding granulomatous reaction with plasma cells numerous in the interstitium. HE × 130

FIG. 9 Two adjacent glomeruli, the one on the left being essentially normal compared with the small, dense, contracted appearance of the affected glomerulus on the right. HE × 250

FIG. 10 Arcuate artery showing fibrinoid necrosis of the media and adventitia and periarterial infiltrates of lymphocytes and plasma cells. HE × 250

FIG. 11 Longitudinal section of arcuate artery with fibrinoid necrosis of media and adventitia illustrating the nodular distribution of the lesions. HE × 125

FIG. 12 Encysted microsporidia (arrow) in interstitium caused no host response as long as cyst remained intact. HE × 1 600

FIG. 13 Dispersal of individual microsporidia (not visible at this magnification) resulting in a granulomatous response composed of histiocytes, endothelioid and epithelioid cells in the interstitium. HE × 130

FIG. 14 Granulomatous reaction in the interstitium sometimes extended up to Bowman's capsule of an unparasitized glomerulus. HE × 250

FIG. 15 Ruptured parasitized renal epithelial cell spilling microsporidia into lumen of tubule. HE × 1 600

FIG. 16 Epithelial cell greatly distended by microsporidia. HE × 1 600

FIG. 17 Collecting tubule lumen filled with both *in situ* and detached parasitized epithelial cells. HE × 250

FIG. 18 Granulomatous reactions in interstitium of the renal medulla. HE × 130

FIG. 19 Glomerular tuft containing 2 cysts filled with microsporidia. Gram × 1 600

FIG. 20 Birefringent spores of microsporidia as photographed under polarized light. Renal epithelial cell. HE × 1 600

FIG. 21 Large numbers of microsporidia in collecting tubules of renal medulla. Gram × 1 600

FIG. 22 Hepatic artery with fibrinoid necrosis and round hole in media due to presence of microsporidia. HE × 325

FIG. 23 Hepatic artery showing segmental fibrinoid necrosis of media and adventitia. HE × 250

FIG. 24 Microsporidia in a hepatocyte. HE × 1 000

FIG. 25 Parasitized Purkinje cell. HE × 425

FIG. 26 Higher magnification showing microsporidia and marginated nucleus of greatly enlarged Purkinje cell. HE × 1 000

FIG. 27 Microsporidia extend into the hillock of this large pyramidal neuron. HE × 1 600

FIG. 28 Parasitized large bipolar neuron. HE × 680

FIG. 29 Large subspherical cyst filled with microsporidia in brain substance. Gram × 1 600

FIG. 30 Similar cyst stained with silver. Note absence of host response. WS × 1 600

FIG. 31 Microsporidia distending small vessels of the brain. HE × 520

FIG. 32 With Gram's stain the microsporidia stand out prominently. Gram × 325

FIG. 33 The cytoplasm of some endothelial cells of vessels in the brain were filled by microsporidia. HE × 520

FIG. 34 A longitudinal section of a vessel in the brain showing the lumen completely occluded by the large number of parasites. HE × 425

FIG. 35 Arteriole in brain with extensive vasculitis and perivasculitis forming cuff around it. HE × 450

FIG. 36 A small blood vessel in the brain showing segmental involvement by fibrinoid necrosis and perivasculitis. HE × 325

FIG. 37 Glial nodule in brain. These nodules were prominent in both grey and white matter. HE × 170

FIG. 38 The small microsporidia easily demonstrable in such glial nodules with an appropriate stain. GRAM × 400

FIG. 39 Fibrinoid necrosis adjacent to blood vessels present in the choroid plexus and accompanied by inflammatory cells. HE × 250

FIG. 40 Focal areas of rarefaction occasionally found in both grey and white matter of the brain. HE × 250

FIG. 41 Russell-Fuchs bodies also occasionally present amongst plasma cells in both grey and white matter. HE × 680

FIG. 42 A vein showing phlebitis and periphlebitis characterized by fibrinoid necrosis and a heavy infiltrate of lymphocytes and plasma cells. HE × 500

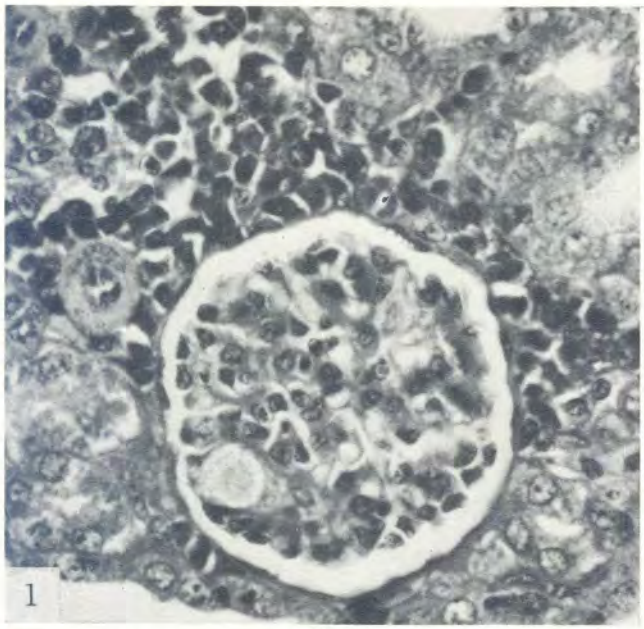
1

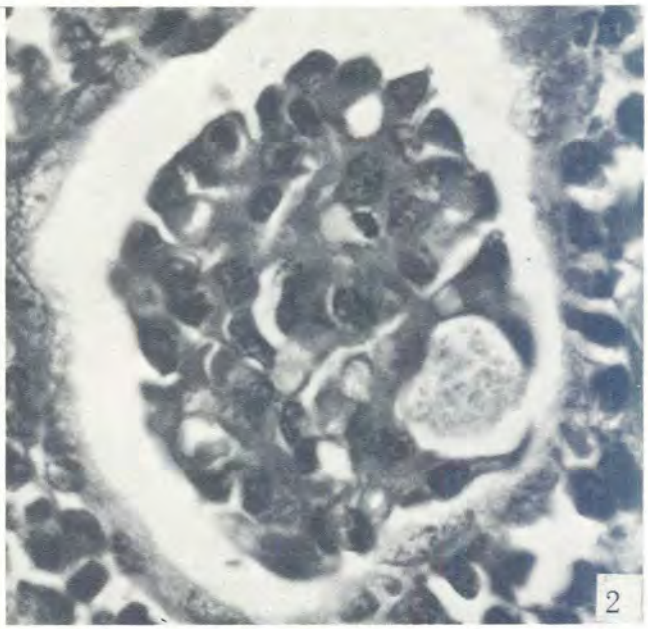
2

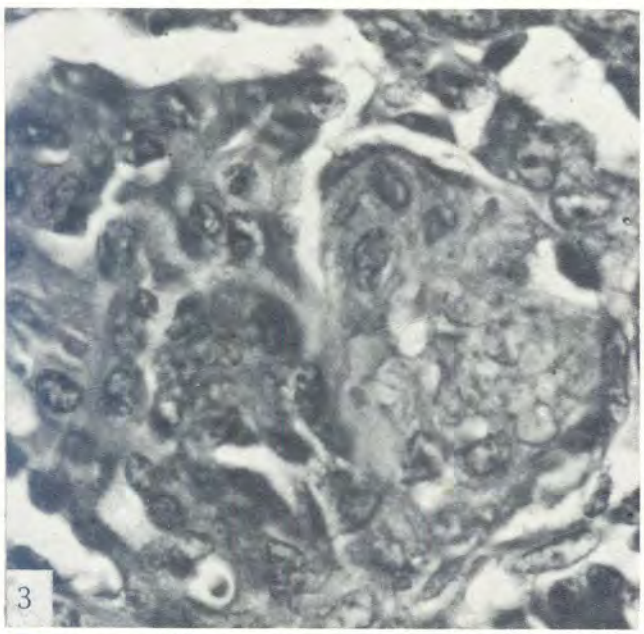
3

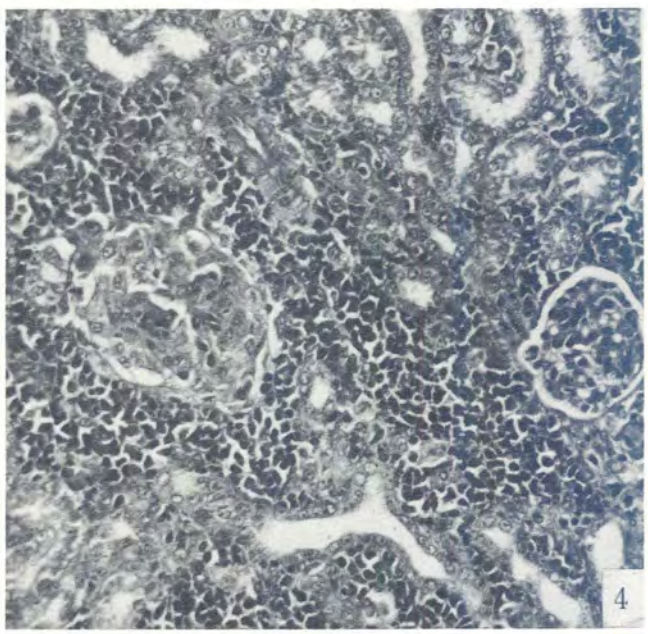
4

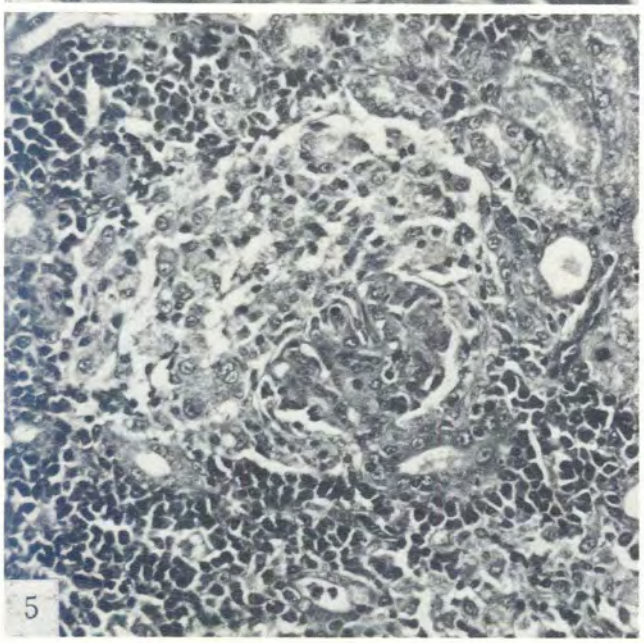
5

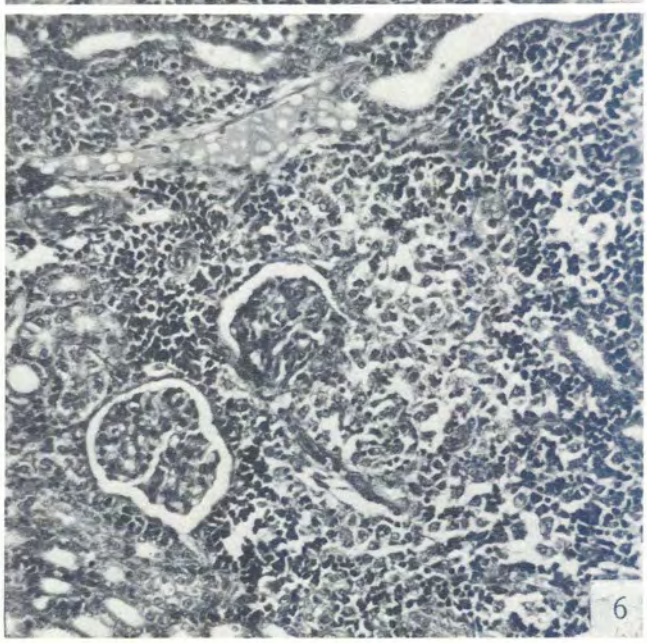
6

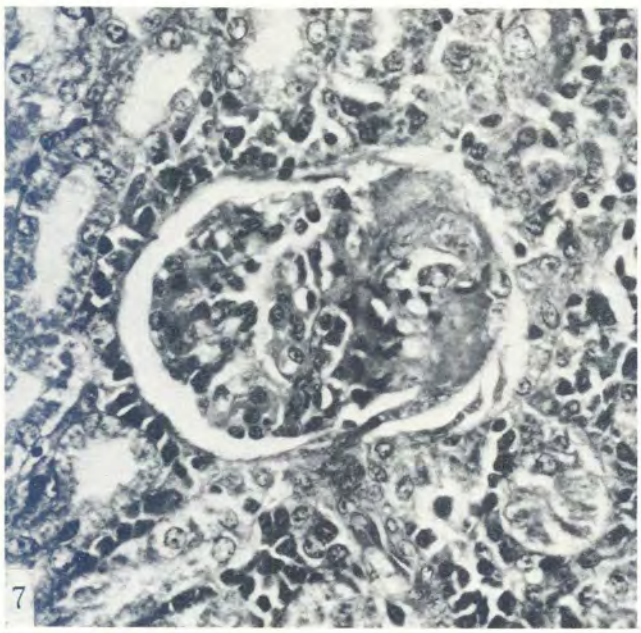
7

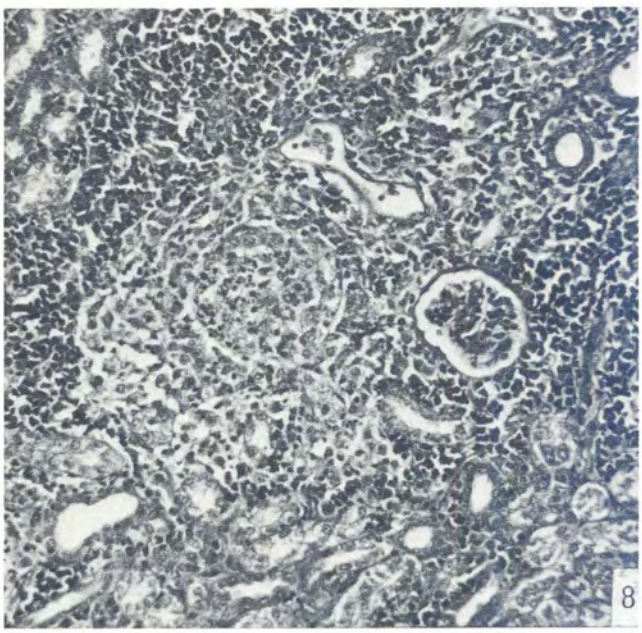
8

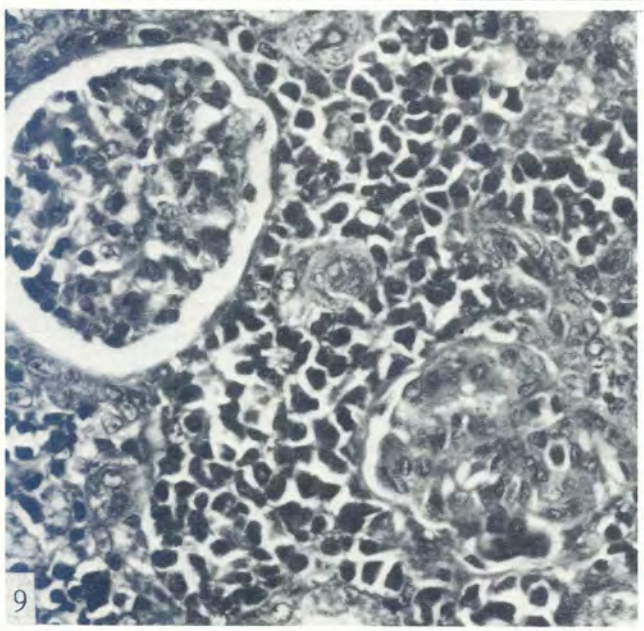
9

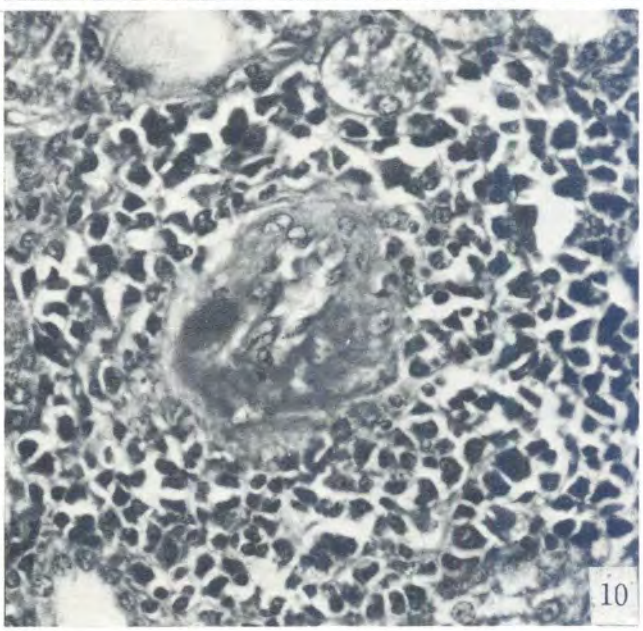
10

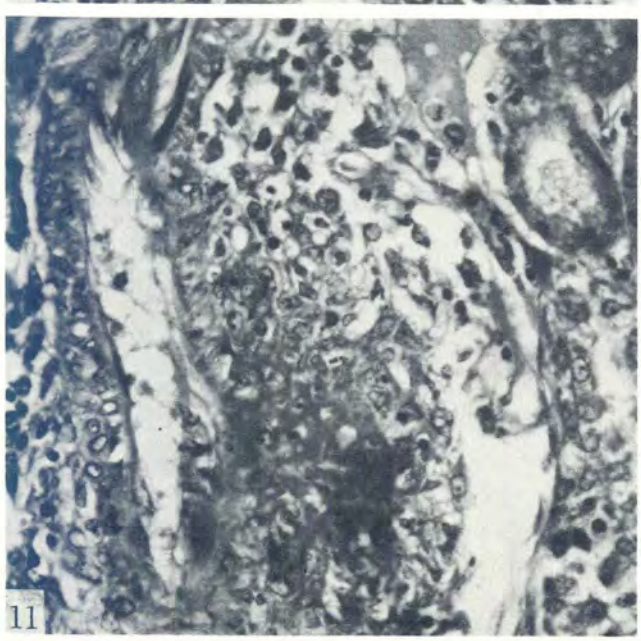
11

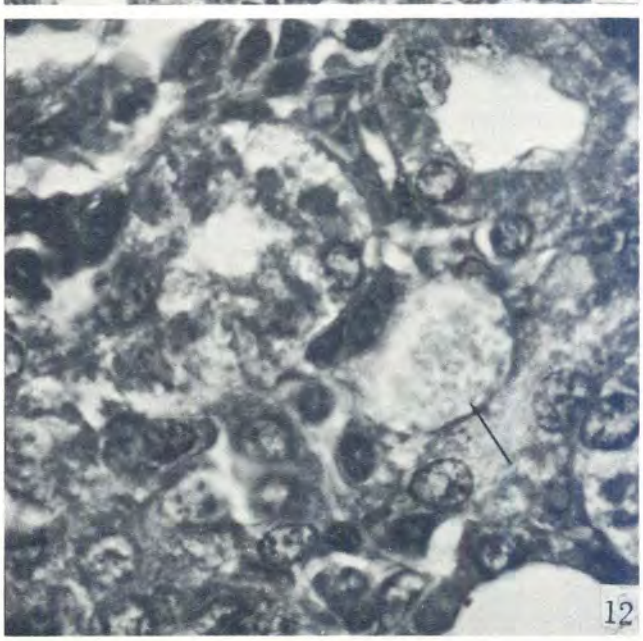
12

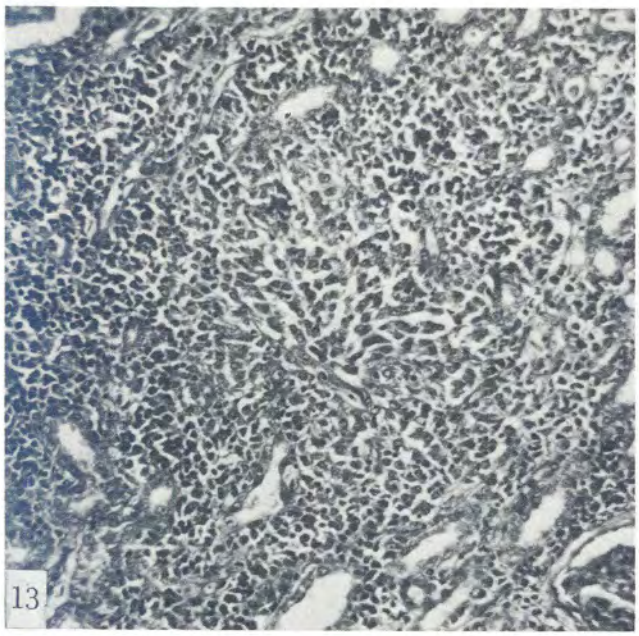
13

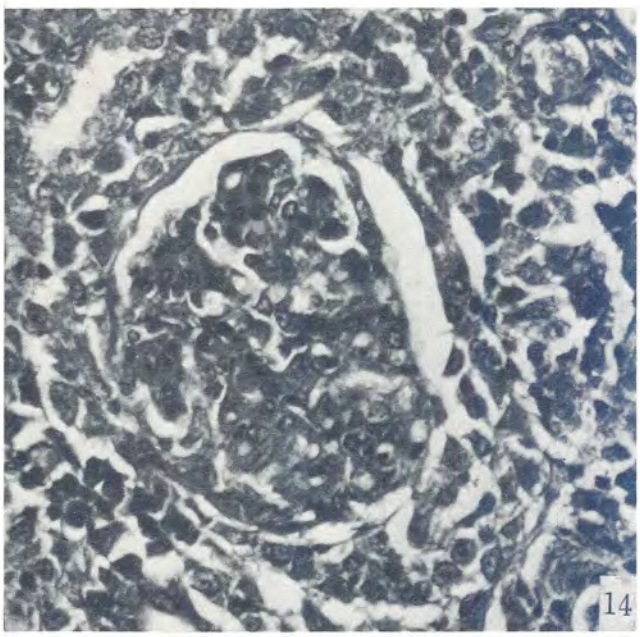
14

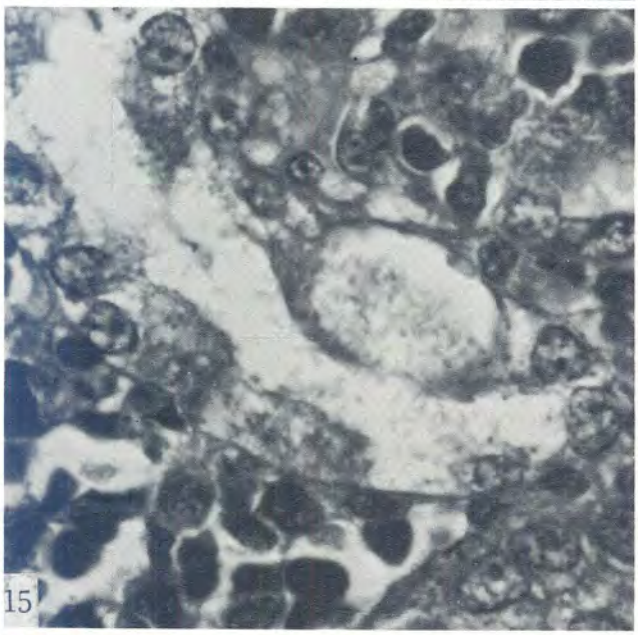
15

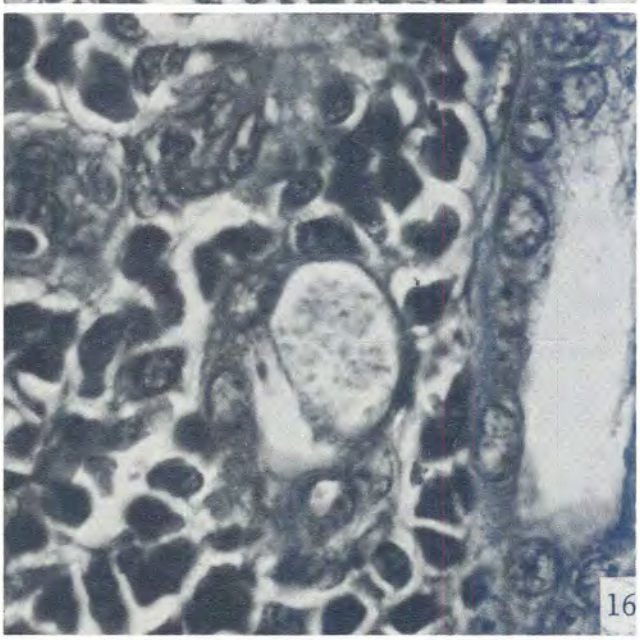
16

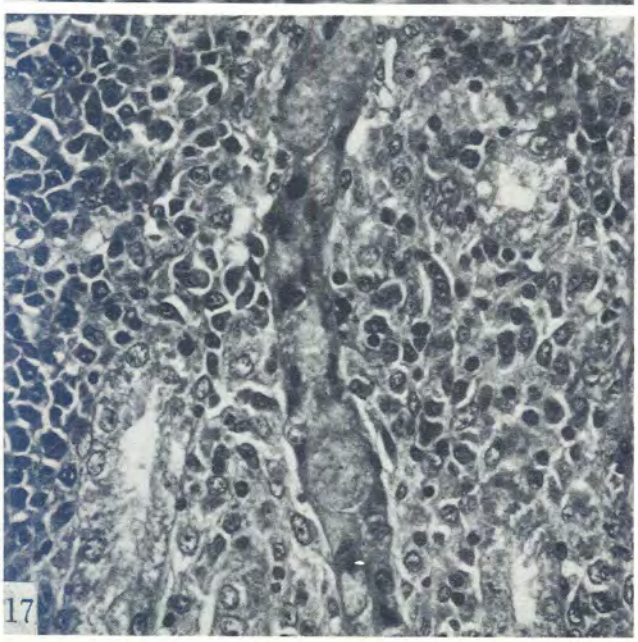
17

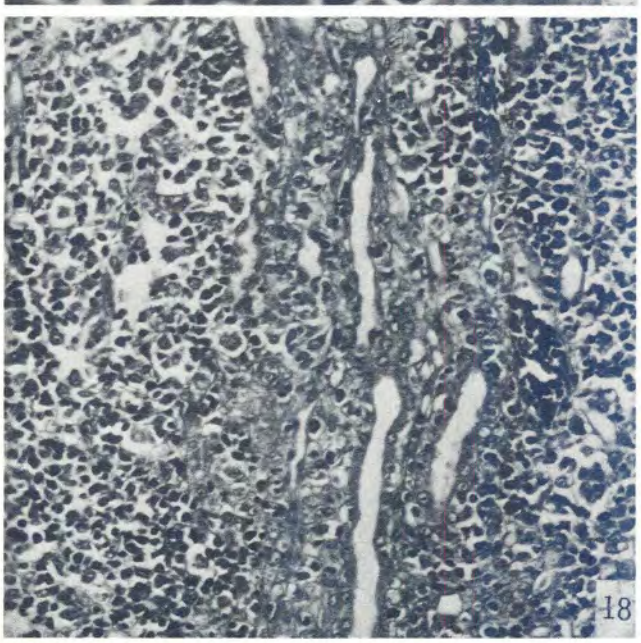
18

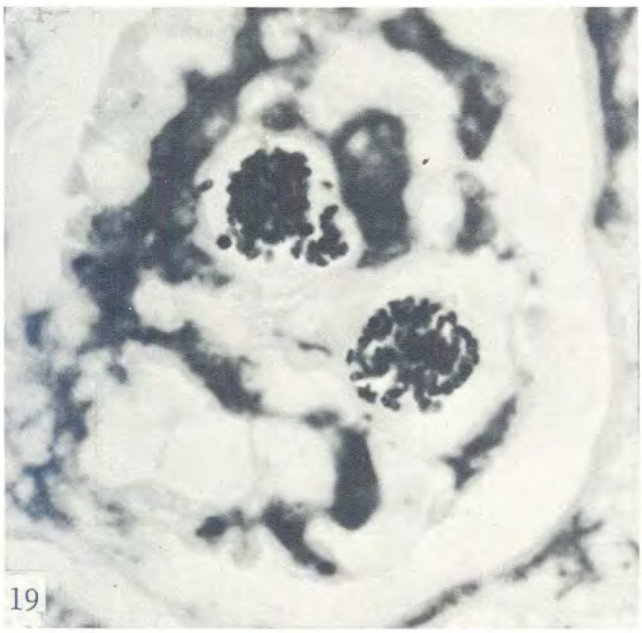
19

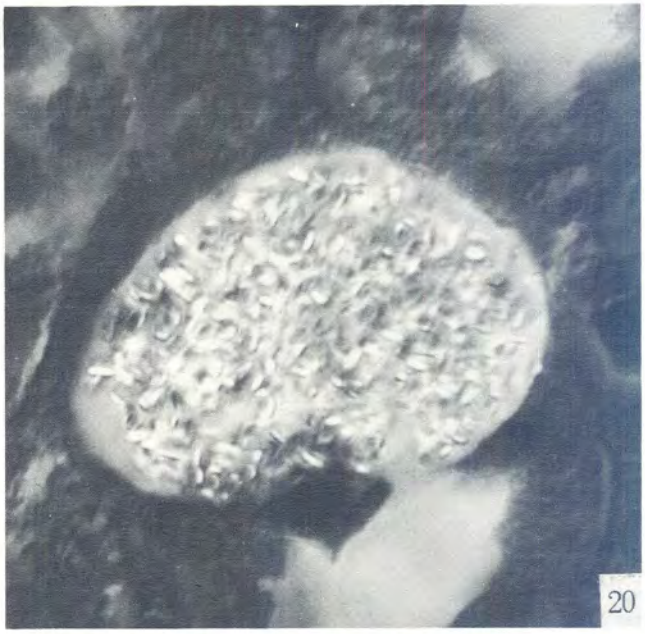
20

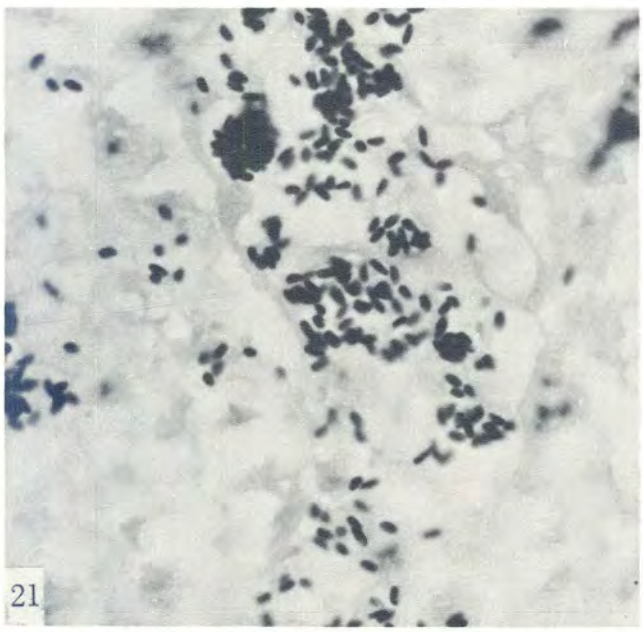
21

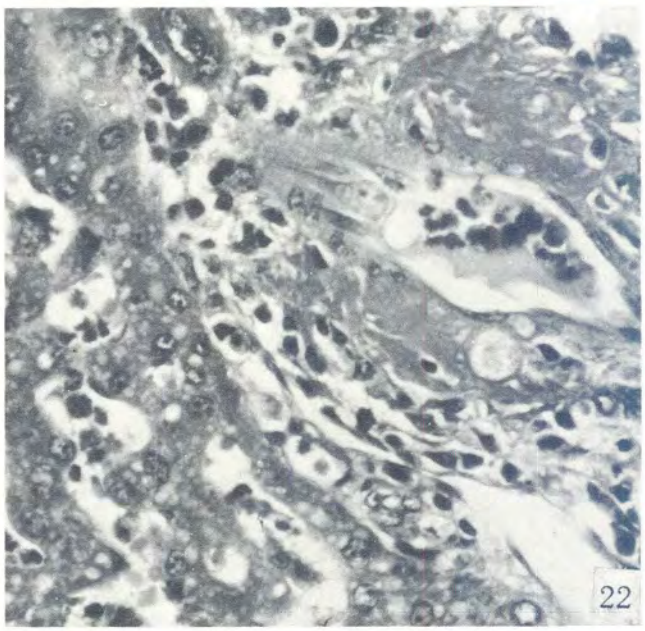
22

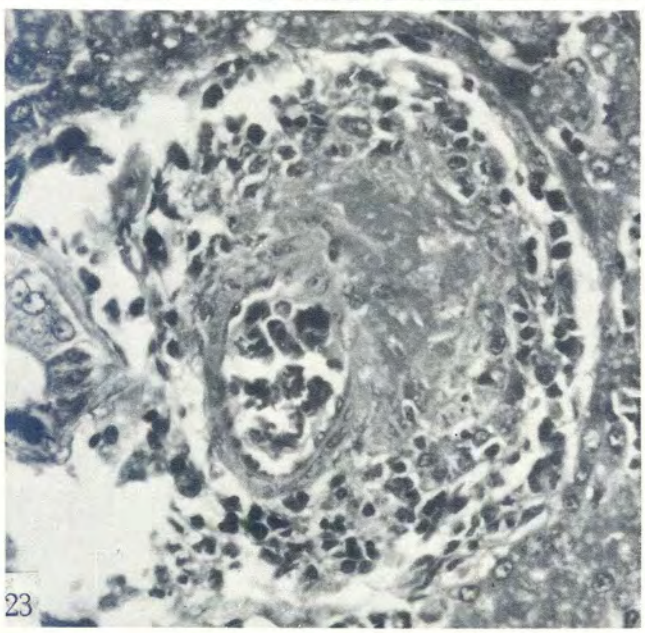
23

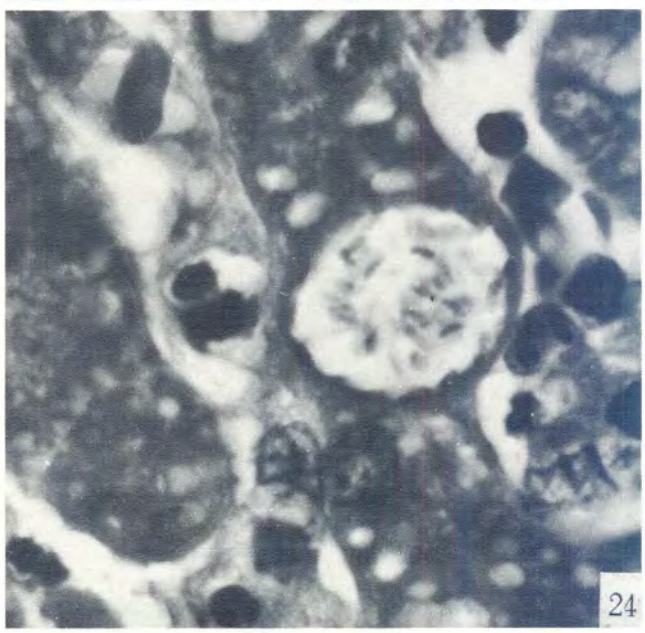
24

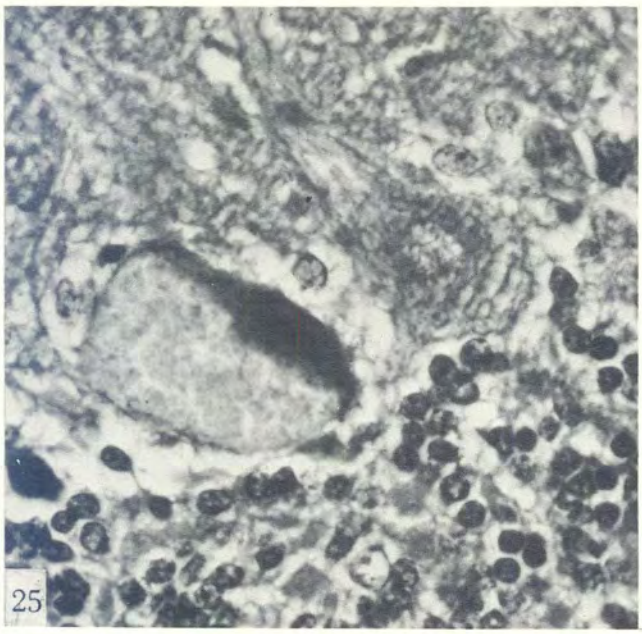
25

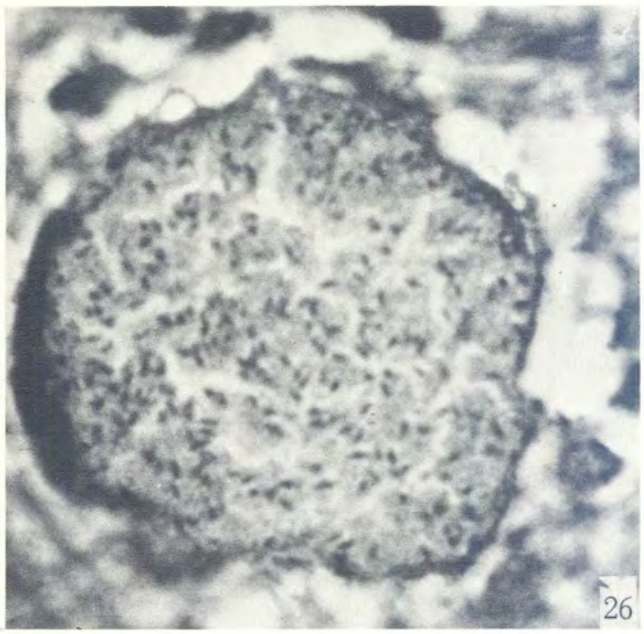
26


27

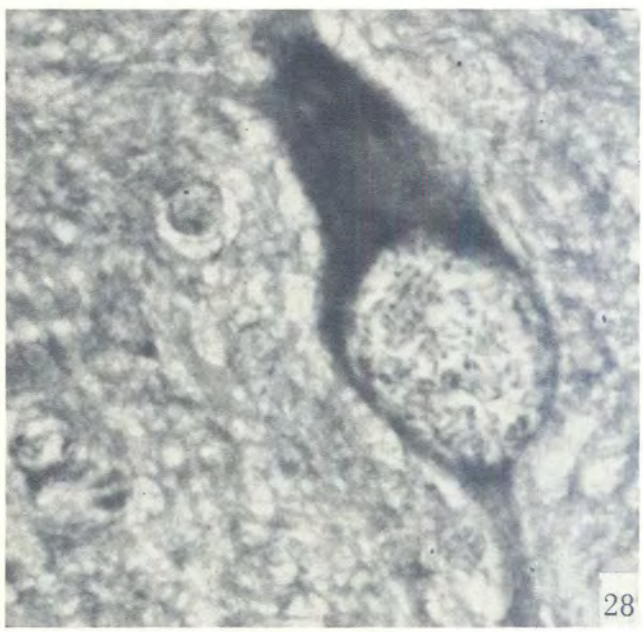
28

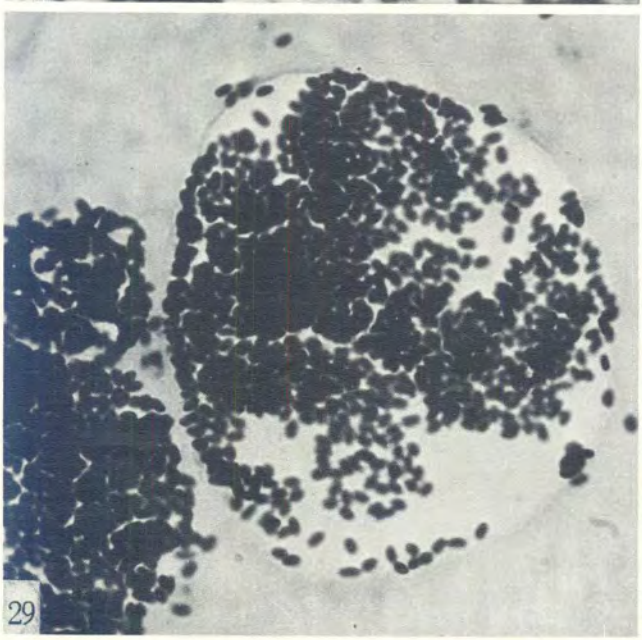
29

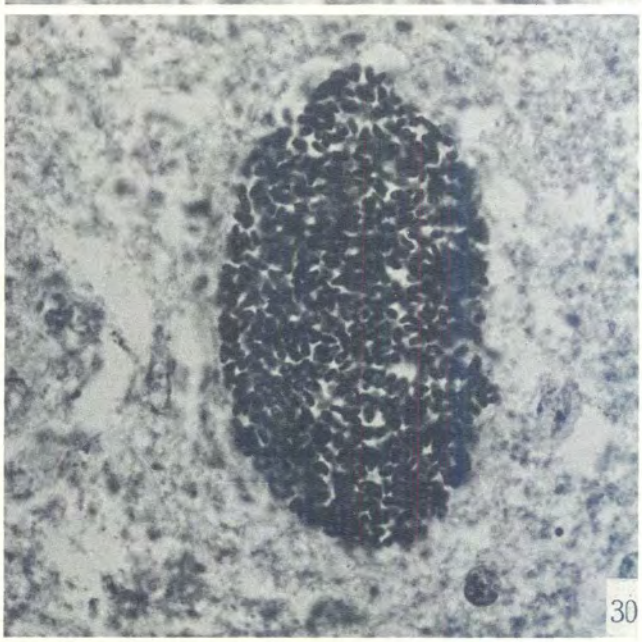
30

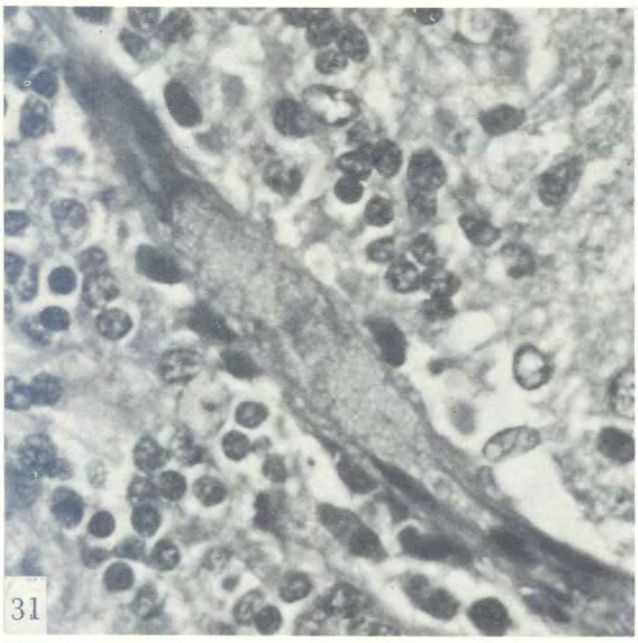
31

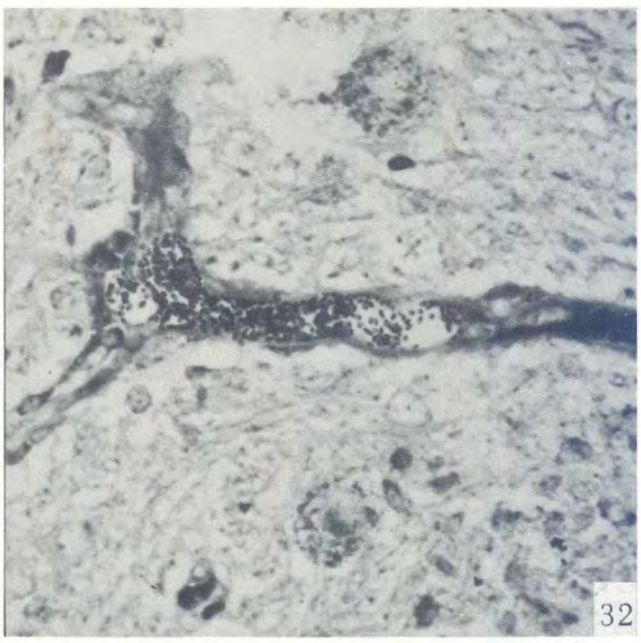
32

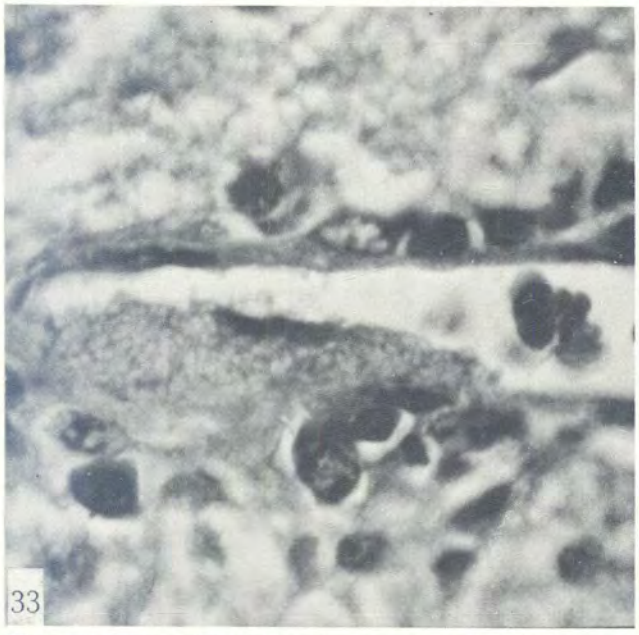
33

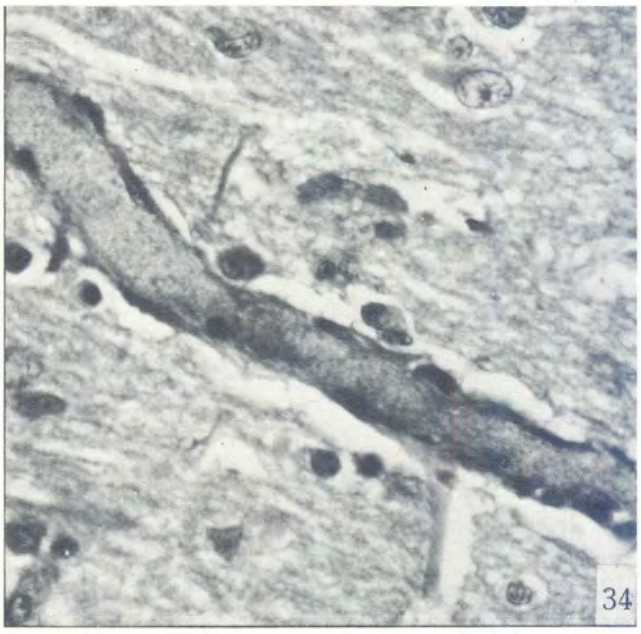
34

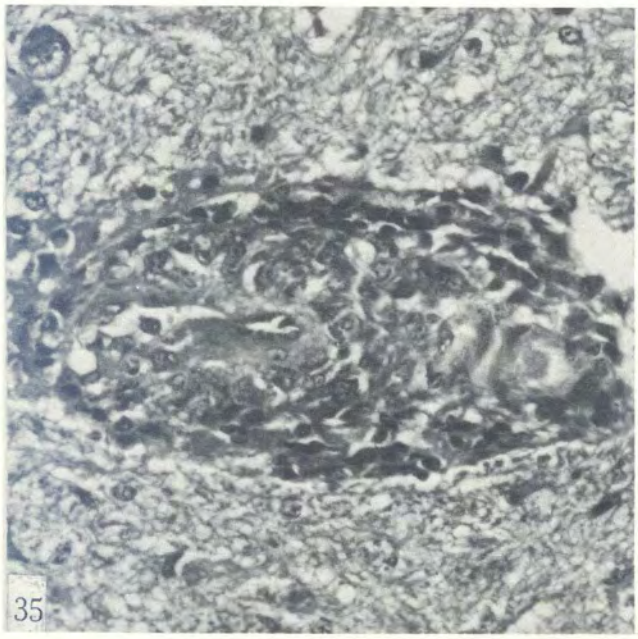
35

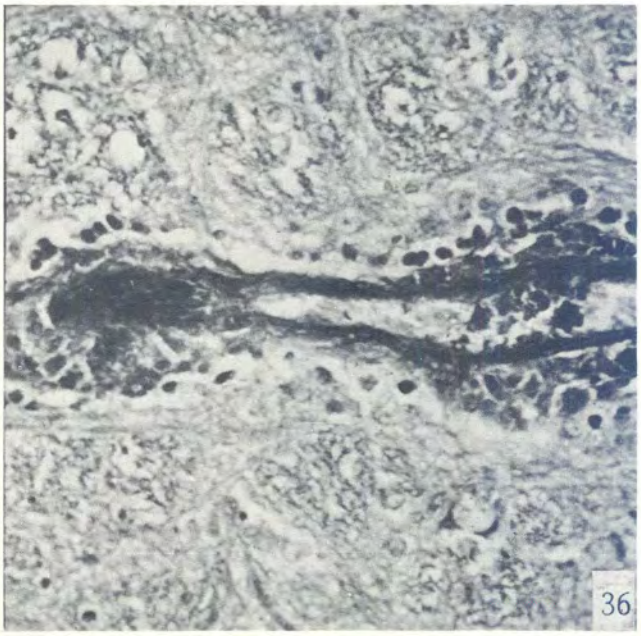
36

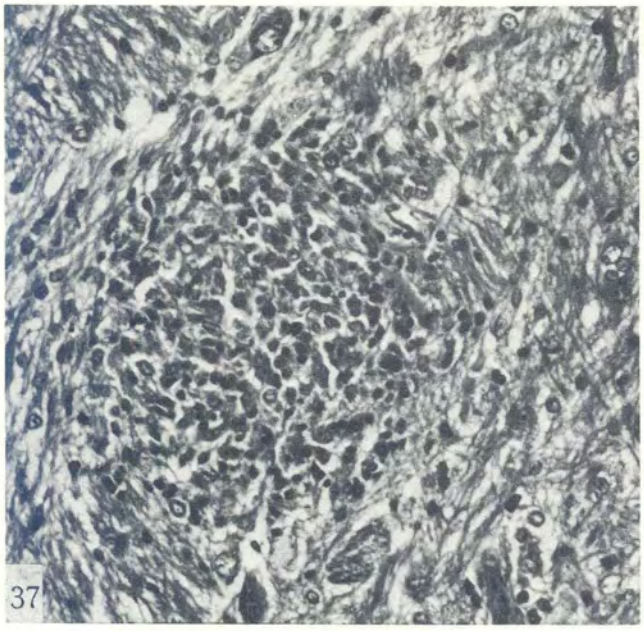
37

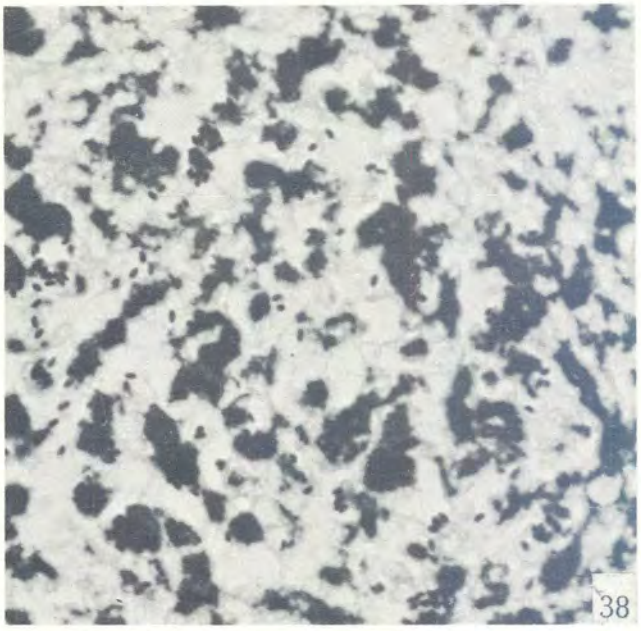
38

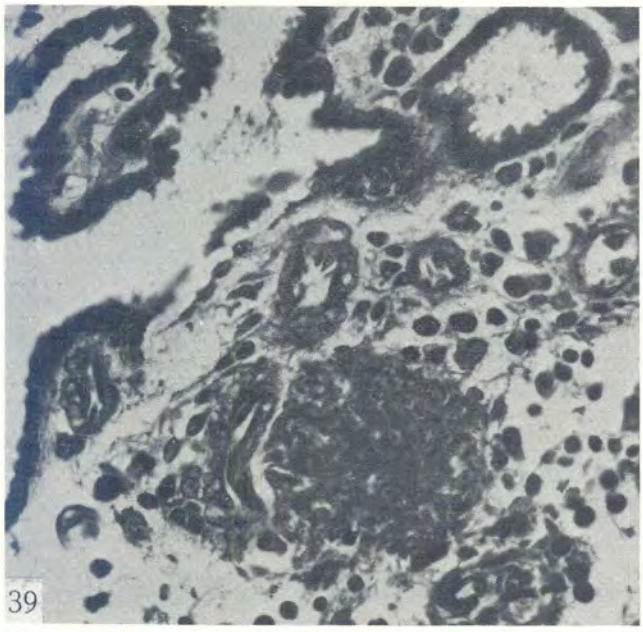
39

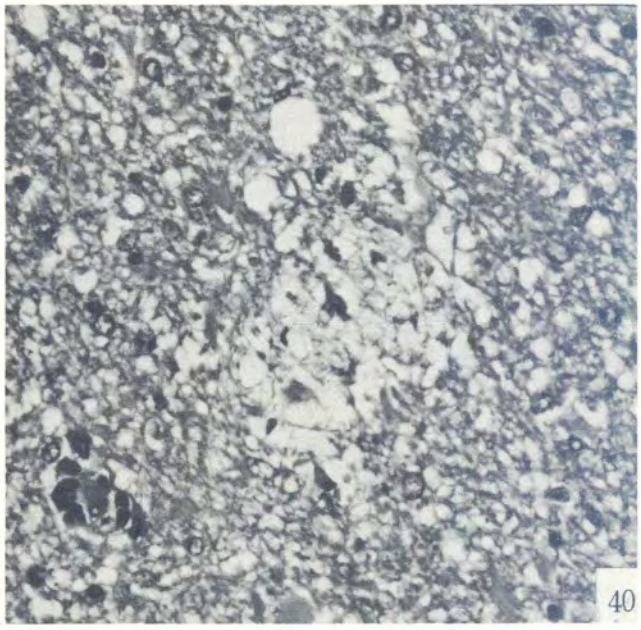
40

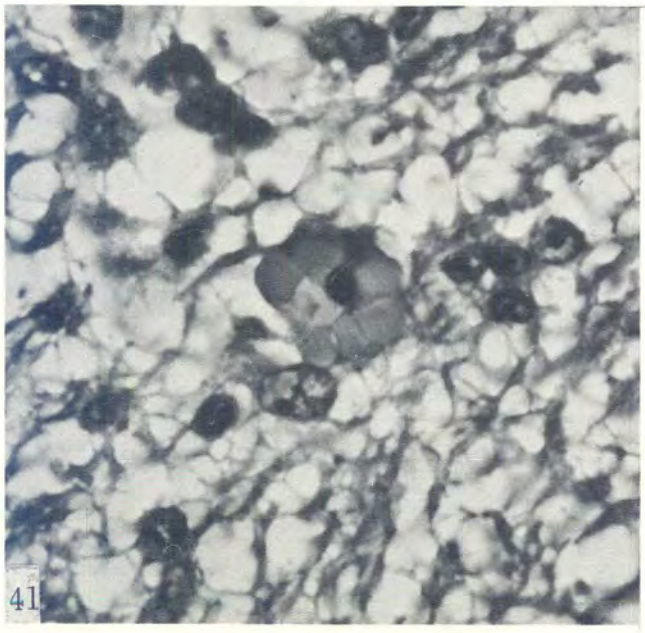
41

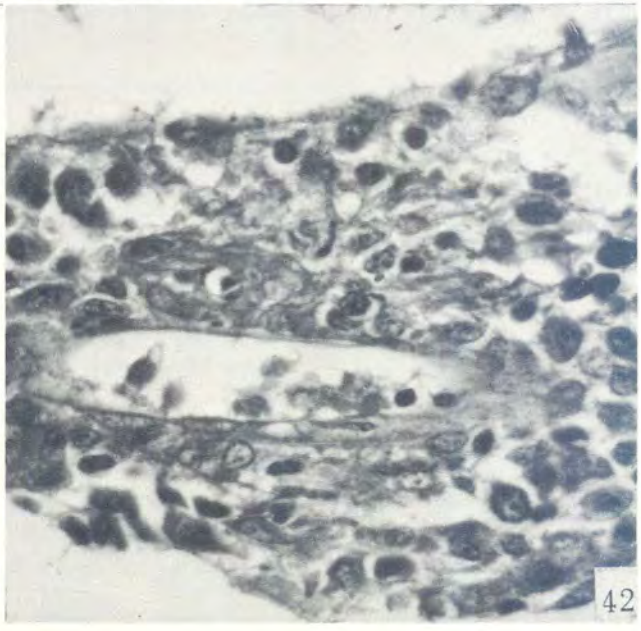
42

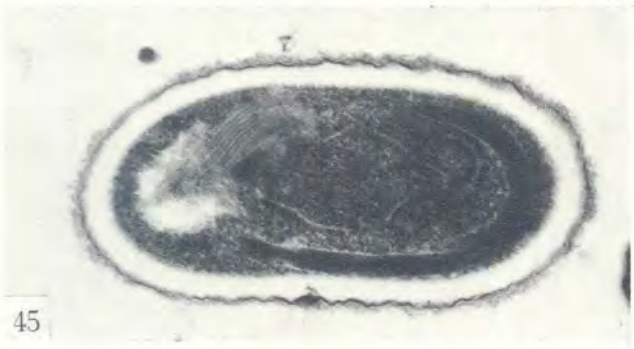

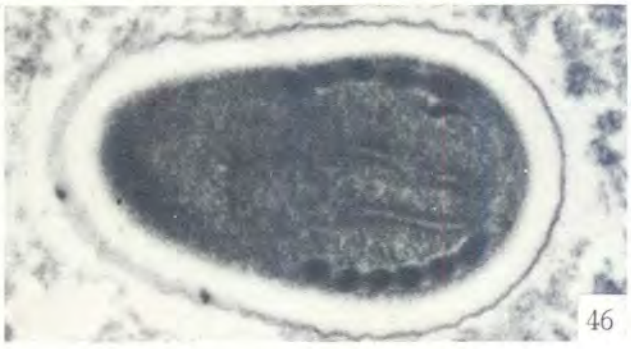

FIG. 43 Kidney. Near cross-sectional view of a mature intracytoplasmic spore in close apposition to the nucleus of a renal tubule epithelial cell. The parasite's nucleus and six coils of filament are clearly visible. ×34 000

FIG. 44 Kidney. Longitudinal view of a mature spore. Note that the polaroplast in the anterior vacuolated pole has the filament passing through its centre. Partial exposure of the nucleus is seen in the posterior pole. Rough endoplasmic reticulum is prominent in the centre of the spore. The dense outer lamina of the anterior part of the spore wall is probably artifactually ruptured. ×35 000

FIG. 45 Kidney. Mature spore showing developing anterior polar vacuole and laminar structures associated with the polaroplast. ×35 000

FIG. 46 Kidney. Mature spore showing cross section of six loops of filament. A nucleus is vaguely discernible. ×32 000

FIG. 47 and 48 Kidney. Cross-sectional and longitudinal view of a microsporidian parasite thought to be a sporont. Note the thickening wall. Organellae are not discernible. ×35 000

FIG. 49 and 50 Kidney. Cross-sectional and longitudinal view of what are undoubtedly sporoblasts. ×142 000

FIG. 51 Brain. Sporoblasts which contain developing organellae. The central organism clearly demonstrates cross sections of a filament with a dense, solid core, and that on the right demonstrates its laminated polaroplast and centrally transversing filament. ×35 000

FIG. 52 and 53 Brain. A poorly preserved single nucleus is present in the sporoblast seen at the top, left of centre of Fig. 52. One of the 4 dark, dense sporoblasts in the upper right of Fig. 53 reveals its developing anterior pole and laminated polaroplast. ×35 000

FIG. 54 Brain. Two sporoblasts with filament and polaroplast easily discernible. The one on the left shows the outline of an apparent single nucleus. ×36 000

FIG. 55 Kidney. Intracytoplasmic, distal, penetrating end of an apparent microsporidian filament. ×10 000

FIG. 56 Brain. Numerous tightly grouped intracytoplasmic spores in juxtaposition to a host cell nucleus in the brain. Orgenellae of the parasite are not seen. ×15 000

FIG. 57 Kidney. Glomerular mesangial cell with intracytoplasmic spores. ×15 000

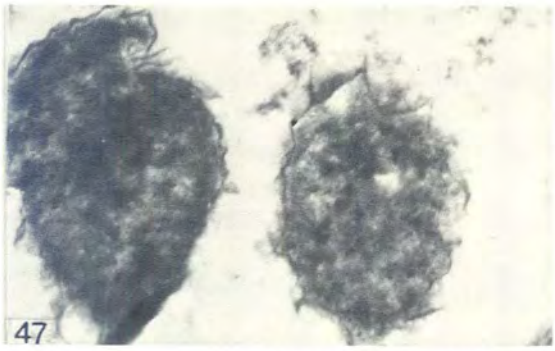
47

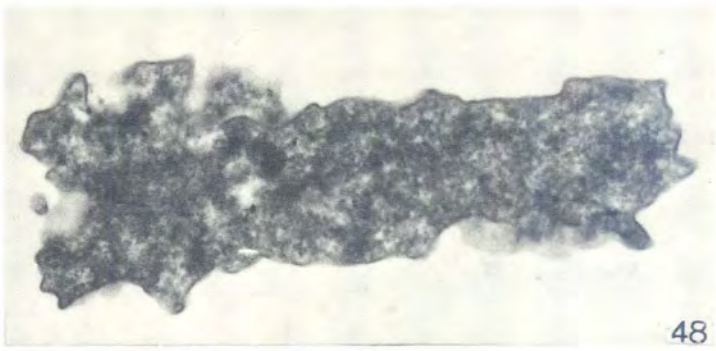
48

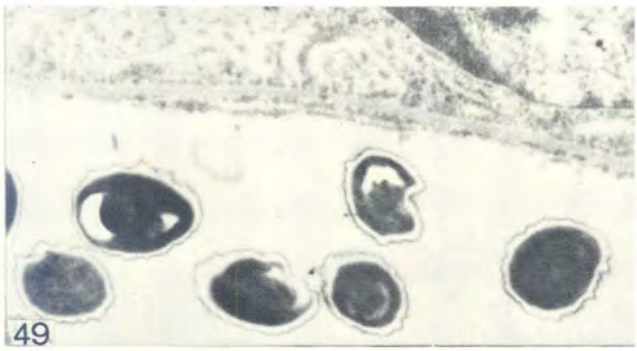
49


50

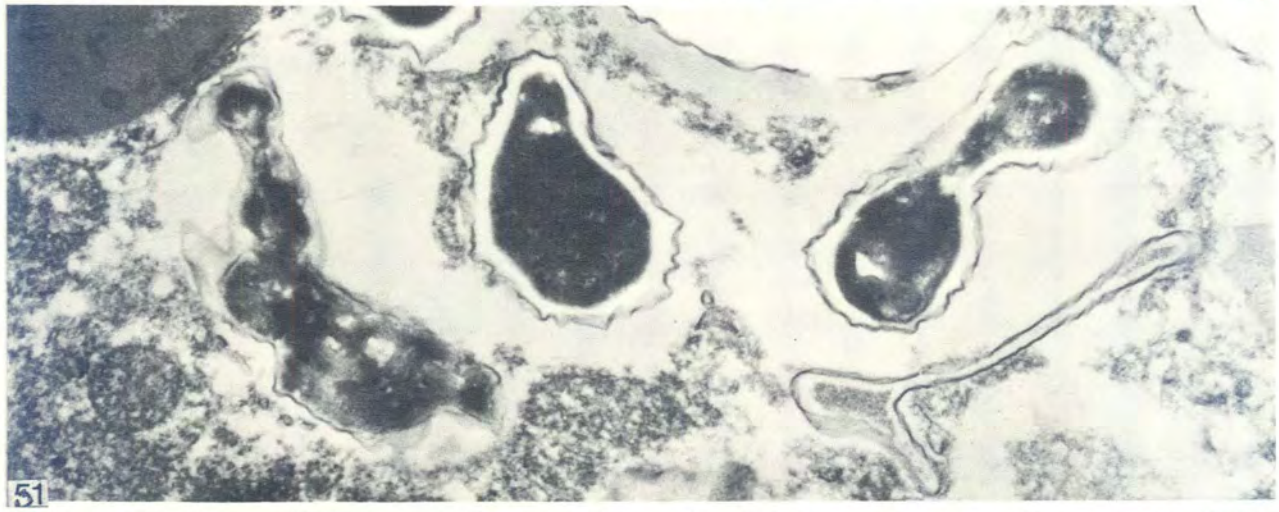
51


52


53

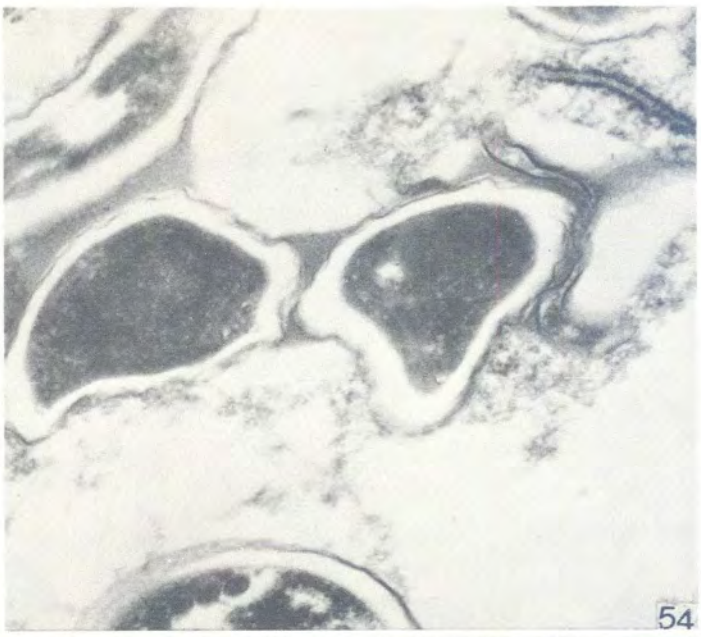
54

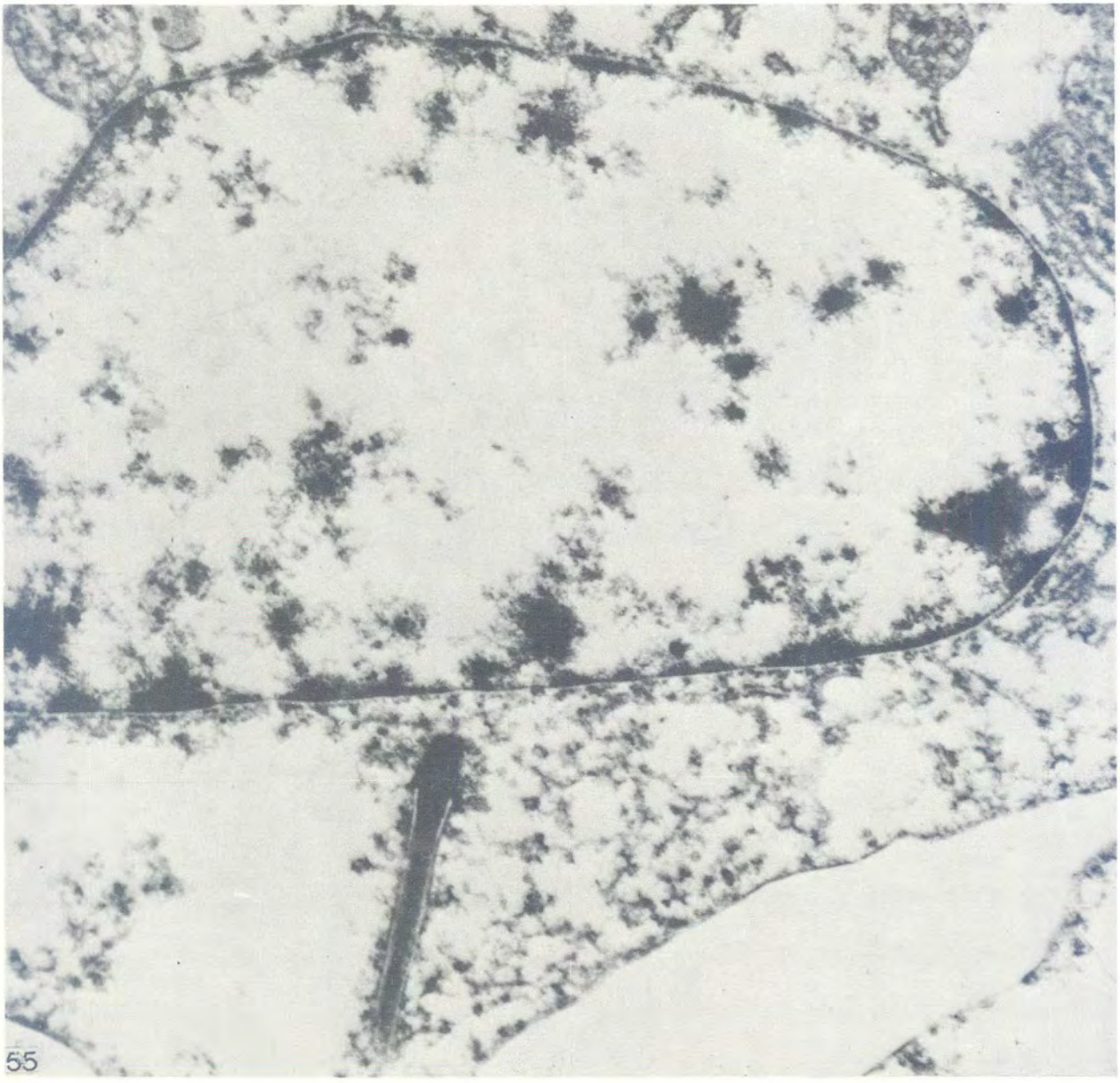
55

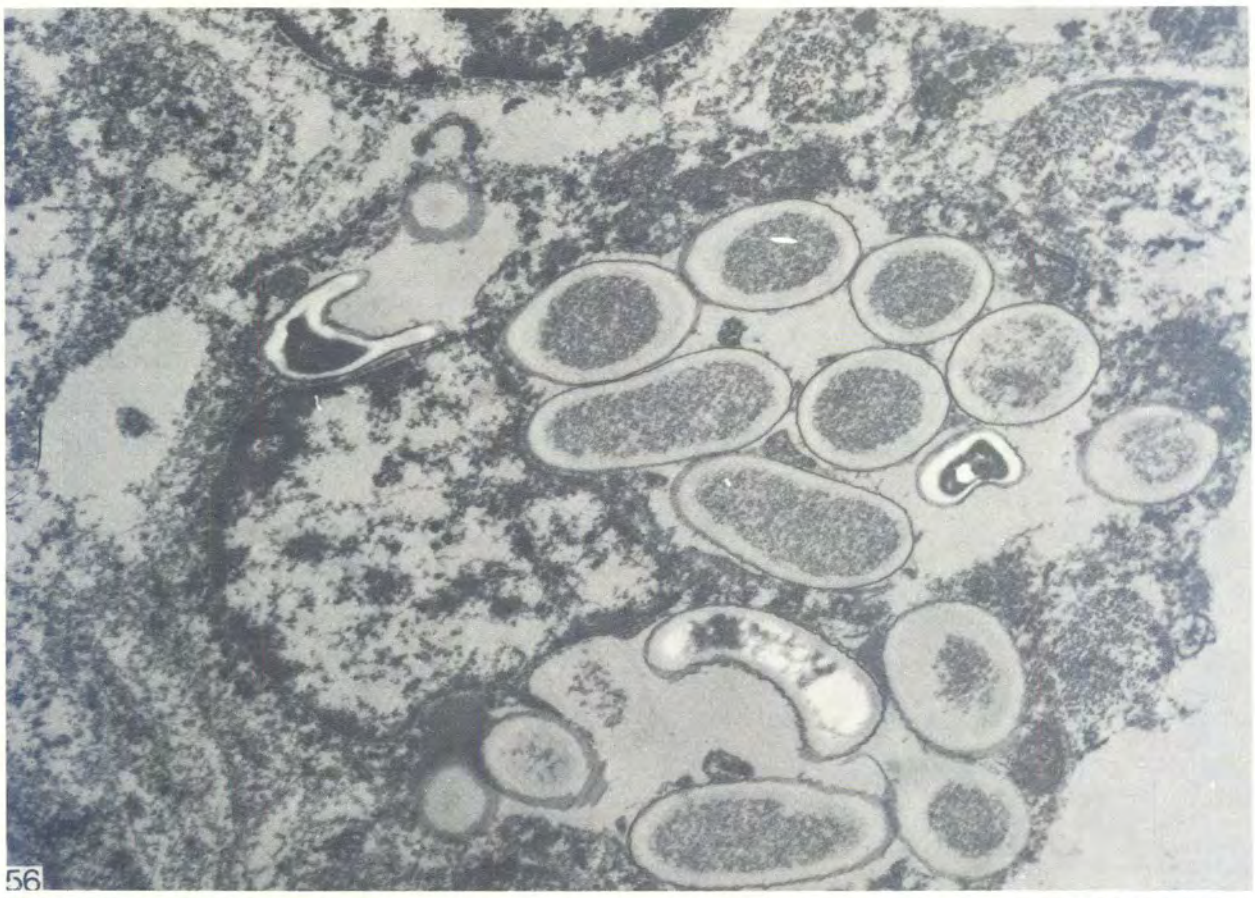

56

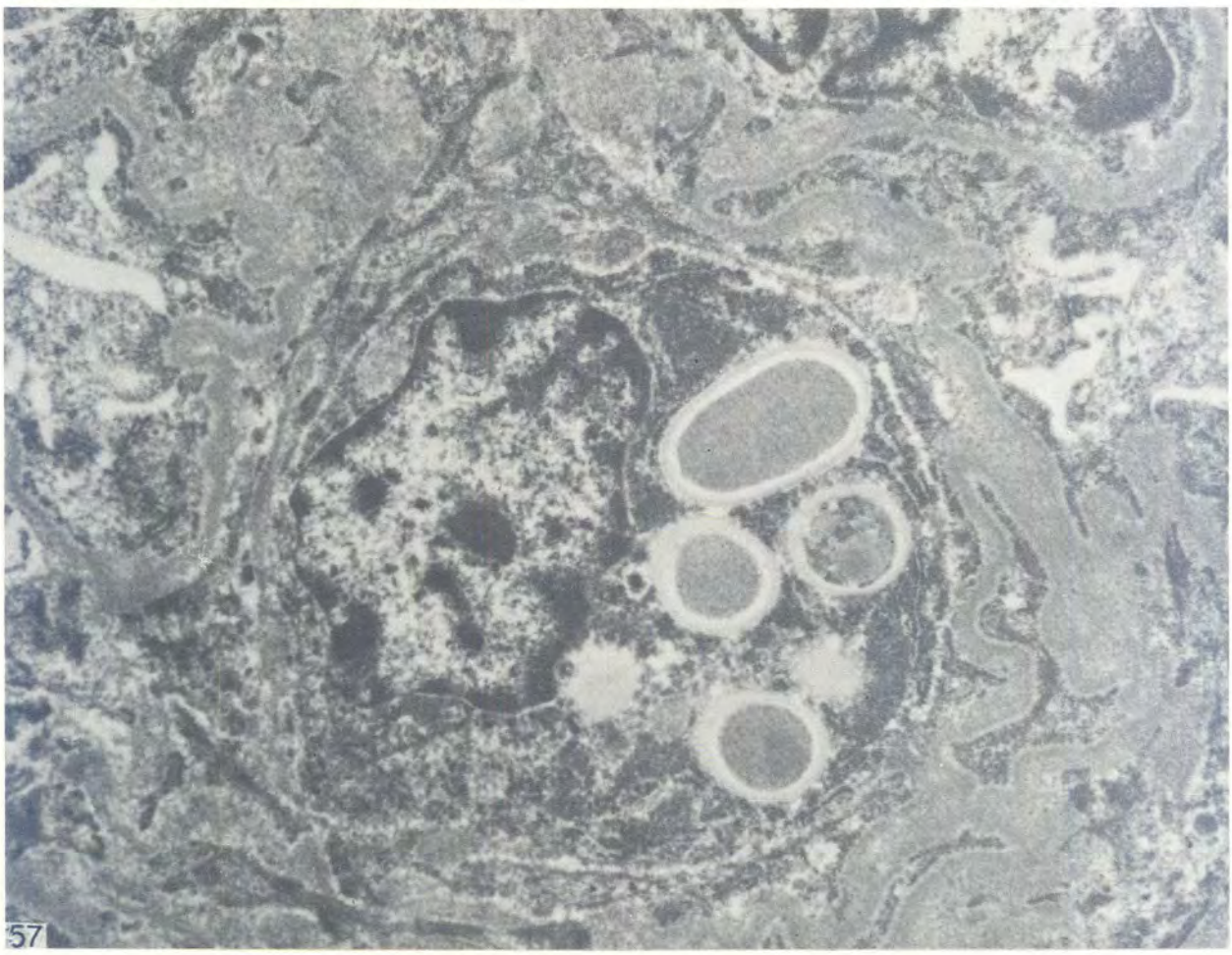

57

Despite the marginal preservation and leached appearance of the host cell, cytoplasmic penetration of an apparent microsporidian filament was preserved and is demonstrated in Fig. 55.

Spores devoid of any recognizable organellae were very numerous in the tissue studied (Fig. 56 & 57). Some of these spores possessed a thin electron-dense, corrugated wall like that found in a mature spore (Fig. 56), and others had a wider, electron translucent wall (Fig. 57). The outer part of the wall was separated from the amorphous internal contents by a wide translucent zone. They were generally of the same size and shape as a normal mature spore and were seen as compact intracellular groups, free in the cytoplasm and not membrane-bound.

Discussion

Several features that are apparently common are described in the available literature on microsporidiosis in dogs. It appears that multiple puppies of a litter are most often affected. Signs of the infection may appear within a few weeks of birth and it would appear that congenital infection is a distinct possibility in dogs. Perrin (1943, cited by Petri, 1969) showed that transplacental infection occurs in mice, and this has also been reported recently in the blue fox (Mohn, Nordstoga & Helgebostad, 1974). Infection of a litter of puppies at an early age from a common environmental source is another possibility, as is infection from the bitch shedding spores in her urine.

Reported clinical signs are primarily referable to the CNS (Plowright, 1952; Plowright & Yeoman, 1952). Puppies show inco-ordination, weakness, abnormal gait, abnormal eye movements and blindness. Others demonstrate changes in their behavioural pattern, exhibiting viciousness, biting, and abnormal voice. Convulsions and seizures are also reported. Microsporidiosis should therefore be considered in the differential diagnosis of diseases of dogs in which there are signs of CNS involvement.

None of the published reports contains information on urine analysis, urea determinations, or other kidney function tests, although it has been suggested that the staining and examination of urinary sediment and intraperitoneal injection of mice with specimens should aid in the clinical diagnosis (Plowright, 1952). It is apparent from this investigation that large numbers of microsporidia are shed in the urine of some cases.

Plowright (1952), who followed the disease in 3 litter mates that became sick simultaneously and died at 68 days, 12 weeks and 7 months of age respectively, showed that the renal lesions are progressive. In the last case the medulla was extensively fibrotic, and the perivascular fibrosis stood out as streaks radiating into the cortex.

Fibrinoid necrosis of the arcuate and hepatic arteries and branches of the spinal and cerebral arteries suggests that the vasculitis may be similar to that of periarteritis nodosa and Aleutian mink disease. Nordstoga (1972) observed similar changes in cases of microsporidiosis in the blue fox (*Alopex lagopus*) and suggested that the parasite had provoked a state of hypersensitivity in many of the foxes.

The microsporidia in the brain seemed to be less developed than those in the kidney. It appeared that most of the organisms in the kidney were acid-fast and birefringent. With few exceptions those in the brain were neither acid-fast nor birefringent. If acid-fastness and birefringency are indications of maturity, then many of the parasites in the brain may represent non-mature organisms, whereas many of those in the kidney may be mature spores. Electron microscopy did not, however, confirm this hypothesis.

There was ample evidence of inadequate fixation for electron microscopy in the present case so that the interpretation of electron micrographs is not altogether reliable. Inadequate fixation is undoubtedly the reason for our inability to find the known proliferative stages, the incomplete morphological details of sporonts and sporoblasts, and the marginal demonstration of nuclear characteristics.

Notwithstanding the handicap this imposes in determining the genus of this organism, indirect evidence suggests that the microsporidian parasite which infected this puppy was a species of the genus *Encephalitozoon*. The apparent presence of a single nucleus and the absence of diplokarya rule out *Nosema*, though they are strong evidence in favour of *Encephalitozoon* (Cali, 1970; Sprague & Vernick, 1971).

The empty spores with and without a dense outer wall are probably either degenerated or poorly fixed spores. The fact that none of these spores was ever seen in the presence of everted polar filaments suggests that they are not germinated spores that have ejected their sporoplasm.

References

BASSON, P. A., McCULLY, R. M. & WARNES, W. E. J., 1966. Nosematosis: Report of a canine case in the Republic of South Africa. *Journal of the South African Veterinary Medical Association*, 37, 3–9.

CALI, A., 1970. Morphogenesis in the genus *Nosema*. *Proceedings of the Fourth International Colloquium on Insect Pathology*, pp. 431–438.

CHANG, S. C., 1972. Hematoxylin-eosin staining of plastic-embedded tissue sections. *Archives of Pathology*, 93, 344–351.

KANTOROWICZ, R. & LEWY, F. M., 1923. Neue parasitologische und pathologisch-anatomische Befunde der nervösen Staupe der Hunde. *Archiv für Wissenschaftliche u. praktische Tierheilkunde*, 49, 137–157.

LEVADITI, C., NICOLAU, S. & SCHOEN, R., 1923. L'etiologie de l'encephalite. *Academie Des Sciences, (Paris)*, 177, 958–988.

LUNA, L. G., 1968. Manual of Histologic Staining Methods of the Armed Forces Institute of Pathology. Third Edition. McGraw-Hill Book Company, New York.

MANOUELIAN, Y. & VIALA, J., 1924. *Encephalitozoon rabiei*, parasite de la rage. *Academie Des Sciences, (Paris)*, 178, 344–345.

MANOUELIAN, Y. & VIALA, J., 1927. *Encephalitozoon negrii*, parasite de l'encephalo-myelite des jeunes chiens. *Academie Des Sciences, (Paris)*, 184, 630–632.

MARGILETH, A. M., STRANO, A. J., CHANDRA, R., NEAFIE, R., BLUM, M. & McCULLY, R. M., 1973. Disseminated nosematosis in an immunologically compromised infant. *Archives of Pathology*, 95, 145–150.

MATSUBAYASHI, H., KOIKE, T., MIKATA, I., TAKEI H. & HAGIWARA, S., 1959. A case of *Encephalitozoon*-like body infection in man. *Archives of Pathology*, 67, 181–187.

MOHN, S. F., NORDSTOGA, K. & HELGEBOSTED, A., 1974. Transplacental transmission of *Nosema cuniculi* in the blue fox (*Alopex lagopus*). *Acta Pathologica Et Microbiologica Scandinavica*, Section B, 82, 299–300.

NORDSTOGA, K., 1972. Nosematosis in blue foxes. *Nordisk Veterinaer Medicine*, 24, 21–24.

PERDRAU, J. R. & PUGH, L. P., 1930. The pathology of disseminated encephalomyelitis of the dog (the "nervous form of canine distemper"). *Journal of Pathology*, 33, 79–91.

PETRI, M., 1969. Studies on *Nosema cuniculi* found in transplantable ascites tumours with a survey of microsporidiosis in mammals. *Acta Pathologica Et Microbiologica Scandinavica*, Supplementum 204.

PLOWRIGHT, W., 1952. An encephalitis-nephritis syndrome in the dog probably due to congenital *Encephalitozoon* infection. *Journal of Comparative Pathology*, 62, 83–92.

PLOWRIGHT, W. & YEOMAN, G., 1952. Probable *Encephalitozoon* infection of the dog. *Veterinary Record*, 64, 381–383.

SCHUSTER, J., 1925. Über eine spontan beim Kaninchen auftretende encephalitische Erkrankung. *Klinische Wochenschrift*, 4, 550–551.

SPRAGUE, V. & VERNICK, H., 1971. The ultrastructure of *Encephalitozoon cuniculi* (Microsporida, Nosematidae) and its taxonomic significance. *Journal of Protozoology*, 18, 560–569.

VAN RENSBURG, I. B. J. & DU PLESSIS, J. L., 1971. Nosematosis in a cat: a case report. *Journal of the South African Veterinary Medical Association*, 42, 327–331.